Research Article

Ireneusz Wlodarczyk*, Kazimieras Černis, and Ilgmars Eglitis

Observational data and orbits of the asteroids discovered at the Baldone Observatory in 2015–2018

https://doi.org/10.1515/astro-2020-0017
Received Jan 01, 2020; accepted Jun 30, 2020

Abstract: This paper is devoted to the discovery of 37 asteroids at the Baldone Astrophysical Observatory (MPC 069) from 2015 to 2018, and one of dynamically interesting Mars-crosser (MC) observed at the Baldone Astrophysical Observatory, namely 2008 LX16. In Baldone Observatory, was independently discovered the Near-Earth Object 2018 GE3 on the image of 13 April 2018. Also, the NEO 2006 VB14 was observed doing its astrometry and photometry. Moreover, we observed asteroids 1986 DA and 2014 LJ1. We computed orbits and analyzed the orbital evolution of these asteroids. 566 positions and photometric observations of NEO objects 345705 (2006 VB14) and 6178 (1986 DA) were obtained with Baldone Schmidt telescope in 2018 and 2019. We detected their rotation period and other physical characteristics. Also, a Fourier transform was applied to determine the rotation period of asteroid 6178 (1986 DA). Value (3.12 ± 0.02)h was obtained. Our observations confirm the previously obtained rotation period P = 3.25h for 2006 VB14.

Keywords: minor planets, asteroids: search, astrometry, orbits

1 Discoveries of minor planets at the Baldone Observatory in 2015-2018

In (Černis *et al.* 2015), we presented the discovered asteroids at the Baldone Observatory in 2008-2013. In this work, we gathered the discoveries of asteroids in period of 2015-2018. Table 1 lists 37 asteroids discovered at the Baldone Observatory, and Table 2 presents statistics and astrometric observations of the asteroids (both new and known) at the Baldone Observatory in 2015-2018.

Table 3 presents high precision orbital elements of discovered asteroids at the Baldone Astrophysical Observatory in 2015-2018. All orbital computations of asteroids were made using the OrbFit software v.5.0.5 and v.5.0.6. In the last version, the NEODyS Team introduced the error weighing model described by Vereš *et al.* (2017), as announced by F. Bernardi on the Minor Planet Mailing List. We used the JPL DE431 Ephemerides with 17 perturbing massive asteroids as was described in Farnocchia *et al.* (2013a,b) and similar to Wlodarczyk (2015).

The orbits of the following asteroids were not computed because of their short observational arc: 2015 TW238, 2015 TN260, 2015 TG350, 2018 RG17 and 2018 TM9. The Minor Planet Center: https://minorplanetcenter.net/db_search and the JPL Small-Body Database Browser: https://ssd.jpl.nasa.gov/sbdb.cgi also do not give orbital elements of these asteroids.

2 Investigation of NEO asteroids 2006 VB14 and 1986 DA

Two NEO type asteroids 2006 VB14 and 1986 DA were successfully observed over seven and five nights respectively in the autumn of 2018 and spring of 2019. There is no previously reported rotation period for 1986 DA in the Asteroid Lightcurve Database (LCDB) and two possible periods for 2006 VB14 was mentioned in paper Skiff *et al.* (2012). Images at Baldone Astrophysical Observatory were captured with a 0.80/1.20 m, f/3 Schmidt telescope and SBIG STX-16803 CCD camera with an array of 4090×4090 pixels. The field-of-view is 53 × 53 arcmin. The plate scale was 0.78 arcsec per pixel in 1×1 binning mode. Photometric data re-

Corresponding Author: Ireneusz Wlodarczyk: Chorzow Astronomical Observatory, 41-500 Chorzow, Poland; Email: astrobit@ka.onet.pl
Kazimieras Černis: Institute of Theoretical Physics and Astronomy, Vilnius University, Saulėtekio al. 3, Vilnius LT-10222, Lithuania; Email: Kazimieras.Cernis@tfai.vu.lt
Ilgmars Eglitis: Institute of Astronomy, University of Latvia, Raina 19, Riga 1586, Latvia; Email: ilgmars@latnet.lv

ductions for the images were done using the MPO Canopus and MaxIM DL programs. GAIA2 R magnitudes are used for thirty reference stars. Through experimentation with different rotation periods using Fourier fitting, the best fit was 3.25 ± 0.02h for the 2006 VB14 and 3.12 ± 0.02h for the 1986 DA. More detailed processing and the result is described in Eglitis (2019). Obtained rotation periods are typical for similar-sized asteroids.

Table 1. List of asteroids discovered at the Baldone Observatory in 2015–2018.

No.	Date of discovery	Designation	Number	Status
1	2015 Oct. 6	2015 TC23		5 opps, 2011-2017 (MPO435109)
2	2015 Oct. 5	2015 TW238		1 d
3	2015 Oct.11	2015 TN260		1 d
4	2015 Oct.11	2015 TO260		2 opps, 2007-2018 (MPOxxxxxx)
5	2015 Oct.11	2015 TQ260		3 opps, 2004-2017 (MPO403103)
6	2015 Oct.11	2015 TG350		1 d
7	2015 Oct.11	2015 TM366		5 opps, 2008-2018 (MPO438021)
8	2017 Sep.25	2017 SV33		2 opps, 2000-2018 (MPO435137)
9	2017 Sep.25	2017 SW33	512962	Numbered object
10	2017 Sep.26	2017 SX33		2 opps, 2013-2018 (MPO435137)
11	2017 Sep.28	2017 SY33	506714	Numbered object
12	2017 Sep.26	2017 SO42		5-day arc (MPO423876)
13	2017 Oct.18	2017 UT9		2 opps, 2013-2017 (MPO431193)
14	2017 Oct.18	2017 UU9		3 opps, 2008-2017 (MPO428368)
15	2017 Oct.19	2017 UO11		5 opps, 2010-2017 (MPO457146)
16	2017 Oct.19	2017 UP11	507546	Numbered object
17	2017 Oct.19	2017 UQ11		66-day arc (MPO431194)
18	2017 Oct.19	2017 UR11		4 opps, 2008-2017 (MPO431194)
19	2017 Oct.19	2017 US11	508671	Numbered object
20	2017 Oct.19	2017 UT11		3 opps, 2008-2017 (MPO431195)
21	2017 Oct.19	2017 UU11		8 opps, 2000-2017 (MPO445151)
22	2017 Oct.19	2017 UV11		2d
23	2017 Oct.19	2017 UW11	508672	Numbered object
24	2017 Oct.19	2017 UX11		5 opps, 2011-2017 (MPO445151)
25	2017 Oct.19	2017 UY11		4 opps, 2005-2018 (MPO431195)
26	2017 Oct.22	2017 UJ15		6 opps, 2006-2018 (MPO434961)
27	2017 Oct.22	2017 UK15		3 opps, 2006-2018 (MPO434912)
28	2017 Oct.22	2017 UL15		2 opps, 2007-2017 (MPO435141)
29	2018 Mar.18	2018 FU25		11 opps, 2002-2018 (MPO445214)
30	2018 Mar.18	2018 FV25		9 opps, 2002-2018 (MPO445214)
31	2018 Apr.10	2018 GU6		5 opps, 2007-2018 (MPO457150)
32	2018 Apr.10	2018 GV6		2 opps, 2016-2018 (MPO448864)
33	2018 Apr.12	2018 GX8		31-day arc (MPO457150)
34	2018 Sep.10	2018 RG17		3d
35	2018 Sep.10	2018 RH17		3d
36	2018 Oct. 6	2018 TL9		32d
37	2018 Oct. 6	2018 TM9		1d

Table 2. Statistics of asteroid discoveries and astrometric observations of the asteroids (both new and known) at the Baldone Observatory in 2015-2018.

Year	Number of asteroid discoveries	Number of asteroid observations	Number of asteroids observed	References
2015	7	315	92	90967, 91854, 92474, 93114, 93768, 94439, 95374, 95856, 96415, 97002
2016	0	337	116	97712, 98789, 99415,99950, 100351, 100690, 101342
2017	21	3798	972	102359, 103149, 104117, 104989, 105343, 105715, 106573, 107170
2018	9	5561	1516	107827, 108759, 109228, 109684, 110175, 110809, 111864
Total	37	10011	2696	

Table 3. High precision orbital elements of discovered asteroids at the Baldone Astrophysical Observatory in 2015-2018. Epoch JD2458800=2019-Nov-13

a (au)	e	i (deg)	Ω (deg)	ω (deg)	M (deg)
(2015 TC23)					
2.429372091	0.182635917	2.9559711	3.356836	355.770222	48.3335455
1.42E−07	4.07E−07	1.37E−05	1.54E−04	1.61E−04	7.80E−05
H = 17.905 ±0.683	rms=0.650″	60 obs.	arc: 2011 08 23.49297 − 2017 01 28.58383		
(2015 TO260)					
3.180625596	0.070887119	11.3953187	22.8498325	31.605917	239.0392477
1.90E−07	2.74E−07	2.43E−05	5.28E−05	1.20E−04	9.93E−05
H = 16.404±0.585	rms=0.8131″	45 obs.	arc: 2007 04 15.29781 − 2018 04 15.31992		
(2015 TQ260)					
3.110348990	0.173711538	2.76876055	13.7152511	26.845571	261.2529686
6.37E−07	2.764E−06	2.163E−05	3.059E−04	1.180E−03	7.396E−04
H = 17.448 ±0.3219	rms=0.5520″	39 obs.	arc: 2004 09 22.41911 − 2017 02 04.56418		
(2015 TM366)					
3.1528697063	0.2302087879	3.88824662	0.4072676	323.3807139	307.92250206
1.225E−07	1.479E−07	2.036E−05	1.839E−04	1.922E−04	6.395E−05
H =16.624 ±0.415	rms=0.7850″	35 obs.	arc: 2008 05 03.32927 − 2019 05 27.32287		
(2017 SV33)					
2.596986975	0.32106217	3.94955805	318.378029	28.90613	198.413018
4.65E−07	6.43E−06	9.95E−06	4.56E−04	2.12E−03	5.91E−04
H =17.909 ± 0.460	rms=0.657″	39 obs.	arc: 2000 08 20.20300 − 2018 01 13.25831		
(2017 SW33) = 512962					
2.49451779180	0.075273159	4.56632761	277.461649	158.269786	148.303396
3.71E−08	2.21E−07	7.43E−06	1.76E−04	4.84E−04	4.46E−04
H =17.415 ±0.327	rms=0.6201″	89 obs.	arc: 2003 02 07.19573 − 2019 03 29.20248		
(2017 SX33)					
2.5864054961	0.208738335	13.8702814	358.2761181	13.259308	191.3409471
7.01E−08	4.13E−07	1.39E−05	4.82E−05	1.02E−04	5.56E−05
H =17.297 ±0. 327	rms= 0.549″	82 obs.	arc: 2013 07 13.58646 − 2018 12 18.61360		
(2017 SY33) = 506714					
3.1085619561	0.150125507	10.86908766	245.9033338	138.5060902	140.4297591
5.12E−08	1.00E−07	9.04E−06	4.02E−05	4.70E−05	2.54E−05
H =16.267±0.353	rms=0.563″	113 obs.	arc: 2006 10 19.26301 − 2019 02 12.22559		
(2017 SO42)					
3.035052	0.298238	10.92025	349.1063	80.2855	120.1744
8.03E−04	1.91E−04	4.36E−03	1.29E−02	6.98E−02	7.92E−02
H =17.573±0.352	rms=0.5584″	20 obs.	arc: 2017 09 26.93260 − 2017 10 27.36415		
(2017 UT9)					
2.58102355	0.32321925	3.8612758	268.176738	138.91726	171.116457
1.39E−06	4.48E−06	4.37E−05	3.36E−04	2.06E−03	9.78E−04
H =19.405± 0.444	rms=0.6059″	87 obs.	arc: 2010 03 29.802647 − 2017 12 13.29233		
(2017 UU9)					
2.6903374450	0.155255830	14.4947483	14.6550361	313.9224434	216.8810519
7.30E−08	1.12E−07	1.56E−05	3.17E−05	5.80E−05	4.90E−05
H =17.121±0.391	rms=0.6392″	69 obs.	arc: 2008 09 28.24006 − 2017 11 26.21166		

Table 3. ...continued

a (au)	e	i (deg)	Ω (deg)	ω (deg)	M (deg)
(2017 UO11)					
3.176691364	0.173435199	12.63523894	266.2553832	23.5723976	226.6515114
3.36E−07	1.47E−07	8.61E−06	4.37E−05	5.34E−05	5.08E−05
H =16.127 ±0.444	rms=0.6059″	87 obs.	arc: 2010 03 29.802647 – 2017 12 13.29233		
(2017 UP11) = 507546					
3.0749347632	0.0967058058	9.26179506	291.7167041	304.0642071	304.9612954
6.56E−08	7.13E−08	8.52E−06	4.59E−05	6.86E−05	5.74E−05
H =15.909 ± 0.507	rms= 0.5669″	115 obs.	arc: 2003 01 13.26051 – 2019 02 04.28338		
(2017 UQ11)					
2.5890834	0.26807656	13.323004	246.266216	182.71100	162.66511
6.38E−05	8.05E−06	5.45E−04	3.72E−04	3.13E−03	6.49E−03
H =18.491± 0.350	rms=0.5018″	52 obs.	arc: 2017 10 19.85910 – 2017 12 25.18959		
(2017 UR11)					
2.6807702145	0.144368736	8.3745189	274.985037	68.862129	216.7027455
7.90E−08	1.90E−07	1.31E−05	1.03E−04	1.25E−04	7.23E−05
H = 17.295+/0.397	rms=0.4823″	43 obs.	arc: 2008 10 01.38272 – 2017 12 13.31628		
(2017 US11) = 508671					
2.3859692487	0.160919366	6.92275620	276.7944511	103.6515975	217.5621420
2.41E−08	2.11E−07	9.24E−06	7.68E−05	9.14E−05	3.35E−05
H =17.337 ±0.563	rms=0.5436″	114 obs.	arc: 2002 09 12.43381 – 2018 01 23.09846		
(2017 UT11)					
2.59732629	0.139300258	9.7035643	263.742980	121.54740	189.74831
1.01E−06	3.57E−07	3.32E−05	1.54E−04	3.63E−03	2.59E−03
H =17.967±0.393	rms=0.4688″	41 obs.	arc: 2008 07 29.25161 – 2008 07 29.25161		
(2017 UU11) = 540601					
3.1212485729	0.0914724915	9.86793636	272.4684567	138.4550631	129.7969135
5.26E−08	7.35E−08	6.86E−06	4.31E−05	6.77E−05	4.79E−05
H =16.194±0.238	rms=0.4567″	168 obs.	arc: 2000 09 27.328970 – 2019 02 28.20925		
(2017 UV11) = (2006 WJ117)					
3.1299502232	0.050543408	9.6165970	275.7779533	47.573128	213.284701
8.66E−08	1.13E−07	1.23E−05	6.48E−05	1.77E−04	1.740E−04
H =16.628 ±0.258	rms= 0.5381″	56 obs.	arc: 2006 11 20.32876 – 2019 01 27.27727		
(2017 UW11) = 508672					
3.059355342	0.0372733466	14.4946777	262.2331278	359.449023	277.760331
1.01E−07	9.38E−08	1.02E−05	3.64E−05	1.36E−04	1.35E−04
H =15.504 ±0.401	rms=0.5756″	127 obs.	arc: 2006 10 19.25716 – 2019 02 04.91132		
(2017 UX11) = 540602					
3.0867105093	0.1108896320	9.027172209	324.5622684	13.0643088	191.9568710
9.94E−08	7.83E−08	8.77E−06	5.55E−05	7.32E−05	4.86E−05
H =16.968±0.325	rms=0.6568″	63 obs.	arc: 2011 08 20.48844 – 2019 01 26.35340		
(2017 UY11)					
2.6950766379	0.272327828	8.5874790	269.3278681	150.146374	157.1553239
3.86E−08	2.49E−07	1.22E−05	7.81E−05	1.61E−04	8.89E−05
H = 17.816± 0.351	rms=0.4170″	68 obs.	arc: 2005 01 19.18452 – 2018 01 13.11370		

Table 3. ...continued

a (au)	e	i (deg)	Ω (deg)	ω (deg)	M (deg)
(2017 UJ15) = (2011 SG28)					
3.0627122526	0.138507738	11.01995247	350.1258159	348.8674783	190.8473306
6.74E−08	1.09E−07	9.39E−06	4.95E−05	6.44E−05	4.29E−05
H =15.957 ±0.418	rms=0.5659″	115 obs.	arc: 2006 09 25.97814 – 2019 01 26.37586		
(2017 UK15) = (2006 SP166)					
3.0474848074	0.205704608	10.5527612	351.8583408	357.0501690	177.3259061
6.56E−08	1.66E−07	1.12E−05	6.45E−05	8.22E−05	4.67E−05
H =16.913 ±0.391	rms=0.5788″	56 obs.	arc: 2006 09 17.32566 – 2019 01 08.45827		
(2017 UL15)					
3.013134824	0.18789344	8.5106036	297.914647	98.275308	147.128418
1.77E−07	1.14E−06	1.36E−05	1.13E−04	2.80E−04	1.69E−04
H = 17.086 ±0.576	rms=0.4856″	63 obs.	arc: 2007 11 11.37123 – 2019 01 08.61476		
(2018 FU25)					
2.1914123016	0.1006641254	3.97948215	78.9752374	173.2489201	127.3655201
1.57E−08	5.79E−08	5.88E−06	8.90E−05	9.38E−05	2.96E−05
H =17.755±0.441	rms=0.6165″	198 obs.	arc: 2002 05 19.29185 – 2019 11 02.36125		
(2018 FV25)					
2.7183800786	0.0241541097	6.77614462	50.6255576	345.198803	283.154546
4.20E−08	9.74E−08	8.06E−06	6.09E−05	1.97E−04	1.94E−04
H = 16.823± 0.363	rms=0.6038″	102 obs.	arc: 2002 10 11.21773 – 2019 05 31.54064		
(2018 GU6)					
2.7878820963	0.218606065	10.01210383	67.9409977	140.3972666	125.1274082
5.75E−08	1.36E−07	7.56E−06	6.28E−05	6.82E−05	2.15E−05
H = 16.754 ± 0.508	rms=0.6777″	125 obs.	arc: 2007 12 19.33995 – 2019 09 28.40951		
(2018 GV6)					
3.1900886	0.1715536	15.7750172	55.993845	176.27059	86.12596
4.11E−05	1.22E−05	3.87E−05	1.51E−04	3.38E−03	1.42E−03
H =16.095 ±0.386	rms=0.5422″	40 obs.	arc: 2016 12 23.50997 – 2018 05 16.33500		
(2018 GX8)					
2.63813	0.217833	15.0376	58.1840	187.5315	111.863
1.13E−03	1.74E−04	1.26E−02	1.13E−02	9.30E−02	1.28E−01
H = 17.289±0.315	rms=0.4752″	27 obs.	arc: 2018 04 12.92206 – 2018 05 14.34588		
(2018 RH17) = (2013 PD57)					
2.7444334717	0.2179115435	8.20401087	253.5321727	73.3951895	126.9271613
5.13E−08	8.56E−08	9.50E−06	6.75E−05	7.57E−05	3.24E−05
H = 16.853 ±0.342	rms=0.3863″	66 obs.	arc: 2009 11 09.31667 – 2019 01 03.28688		
(2018 TL9)					
3.066276	0.2399989	5.612387	326.44650	12.5613	111.50667
2.30E−04	8.83E−05	1.29E−04	2.38E−03	1.28E−02	5.88E−03
H = 16.927±0.241	rms=0.3786″	27 obs.	arc: 2018 10 06.91471 – 2019 01 03.36384		

Asteroid 345705 (2006 VB14) was discovered by Catalina Sky Survey on 2006-11-15. According to the orbit classification, it is an Aten-type asteroid and Near-Earth Object. The Minor Planet Center published 1167 of its observations over the interval: 2006-11-15.41375 – 2019-01-08.13551. The first observation was published on 2006-11-15.41375 by (704) Lincoln Laboratory Experimental Test Site (ETS), New Mexico, in the Minor Planet Supplement (MPS) 187233. The first observation by the Astrophysical Observatory in Baldone was made on 2018-10-14.05185 069, MPS 930858. Together, Baldone published 99 astrometric observations of 345705 (2006 VB14).

The second asteroid, 6178 (1986 DA), was discovered at Shizuoka Observatory on 1986-02-16 by M. Kizawa. According to the Minor Planet Center (MPC), asteroid 6178 (1986 DA) has Amor orbit type and belongs to so-called 1+ KM Near-Earth Object.

MPC published 1039 total astrometric observations over interval: 1977-07-17.67267 – 2019-07-30.295697. The first observation was made on 1977-07-17.67267 by (413) Siding Spring Observatory, MPC 24035. The Baldone Astrophysical Observatory (BAO) made the first observation of this object on 2019-04-17.84924, (MPS) 991243. Together, the BAO published 33 astrometric observations of 6178 (1986 DA).

We computed residuals, RMS equal to 0.381" for observations of asteroid 345705 (2006 VB14) using total 1168 observation from which 1164 were selected. Similarly, for asteroid 6178 we have 1041 observations with 1039 selected with RMS=0.479". Due to the long observational arcs, about 12 years and 42 years, respectively, it was possible to compute the non-gravitational parameter $A2$.

Parameter $A2$ depends on the Yarkovsky effect. The Yarkovsky effect is the thermal re-emission of absorbed solar radiation. The non-gravitational acceleration arises from the anisotropic re-emission at thermal wavelengths of absorbed solar absorption. The Yarkovsky effect acts on the semimajor axis, a. The drift of semimajor axis, da/dt depends on the obliquity y of the asteroid, the bulk density ρ, and diameter D of the asteroid (Chesley *et al.* 2014):

$$\frac{da}{dt} \sim \frac{cos(y)}{\rho D} \tag{1}$$

Next, according to Farnocchia *et al.* (2013a, p. 9) we averaged the Yarkovsky effect as a transverse acceleration, a_t=A_2/r^2, where r is heliocentric distance and A_2 is a function of the physical quantities of the asteroid. Then, according to Farnocchia *et al.* (2013b), the semimajor axis drift of asteroid is

$$\frac{da}{dt} = \frac{2A_2(1-e^2)}{np^2} \tag{2}$$

where e is the eccentricity, n is the mean motion and p is the semi latus rectum. As it was shown in Farnocchia *et al.* (2013a), A_2 can be computed either using physical parameters of an asteroid or by fitting observation. The last method is used when we have computed the orbit of an asteroid with small uncertainties. Then, we solved seven orbital parameters instead of the previously six. The NEODyS team have developed the software OrbFit v.5.0 (http://adams.dm.unipi.it/~orbmaint/orbfit/) which computed non-gravitational parameter da/dt or A_2. We used this publicly available software and computed non-gravitational parameter.

Table 4 presents the starting orbital elements of the asteroids 345705 (2006 VB14) and 6178 (1986 DA) computed with the non-gravitational parameter $A2$ and using the same method as in computing results in Table 3. A negative value of $A2$ of asteroid 345705 (2006 VB14) denotes that the mean semimajor axis drifts da/dt<0 and hence the asteroid can be retrograde rotator; in contrary, the positive value of $A2$ of asteroid 6178 (1986 DA) denotes that the mean semimajor axis drifts da/dt>0 and hence asteroid can be a prograde rotator. We can see that the orbital elements have small errors and the non-gravitational parameters $A2$ have typical values as for NEAs computed by Wlodarczyk (2019a,b).

3 2008 LX16 - an asteroid with Mars-crosser type orbit

The asteroid 2008 LX16 belongs to the Mars-crosser type of asteroids, comprising 14637 members as of 27 November 2019, according to the Minor Planet Center states: https://minorplanetcenter.net/db_search/show_by-_orbit_type?utf8=✓&orbit_type=5.

On the other hand, the JPL Small-Body Database lists 17354 of orbital-class Mars-crosser-asteroids: https://ssd.jpl.nasa.gov/sbdb_query.cgi#x. According to the JPL: https://ssd.jpl.nasa.gov/sbdb.cgi#top Mars-crossing Asteroids, or Mars-crossers, are asteroids that cross the orbit of Mars constrained by (1.3 au < q < 1.666 au; a < 3.2 au).

According to https://ssd.jpl.nasa.gov/sbdb.cgi#top the Mars-crossing asteroid 2008 LX16 has absolute magnitude, H = 19.0.

According to the MPC asteroid 2008 LX16 was first observed at Siding Spring Survey on 2008-06-15. Its orbit type is Mars-crosser. The MPC published 139 total astrometric observations over interval: 2008-06-15.52931 – 2018-07-16.34009. The first observation was made on 2008-06-15.52931 by (E12) Siding Spring Survey, MPS 251702. First observation at Baldone was made in 2018-04-12.91523, MPS

Table 4. Initial nominal orbital elements of the asteroids 345705 (2006 VB14) and 6178 (1986 DA): a denotes semimajor axis, e - eccentricity, angles i, Ω and ω refer to the Equinox J2000.0, M - mean anomaly. Epoch: JD2458800.5 TDB = 13 November 2019. Orbital elements are computed with the non-gravitational parameter $A2$.

a (au)	e	i (deg)	Ω (deg)	ω (deg)	M (deg)
345705 (2006 VB14)					
0.7669388731	0.42123761	31.024613	258.7275473	346.441171	314.203021
6.2E–09	1.0E–07	1.5E–05	2.8E–06	1.7E–05	3.3E–05
Orbital parameter: non-gravitational					
$A2$=(–1.19±1.26)E-14 au/d^2					
6178 (1986 DA)					
2.822145979	0.5818043231	4.3052158	64.636860	127.386722	39.4555013
2.1E–08	2.2E–08	5.0E–06	6.6E–05	6.6E–05	3.8E–06
Orbital parameter: non-gravitational					
$A2$=(+3.24±2.98)E-14 au/d^2					

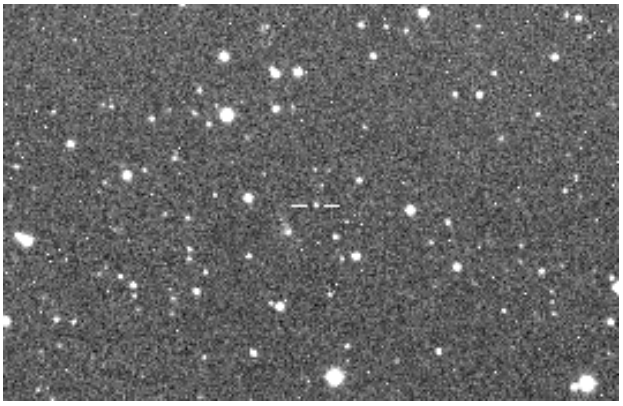

Figure 1. One of the first CCD image of the asteroid 2008 LX16. The size of field is 7 arcmin x 10 arcmin. The image (480 s exposure) taken at the Baldone Astrophysical Observatory with the Schmidt telescope on the night April 19 of 2018.

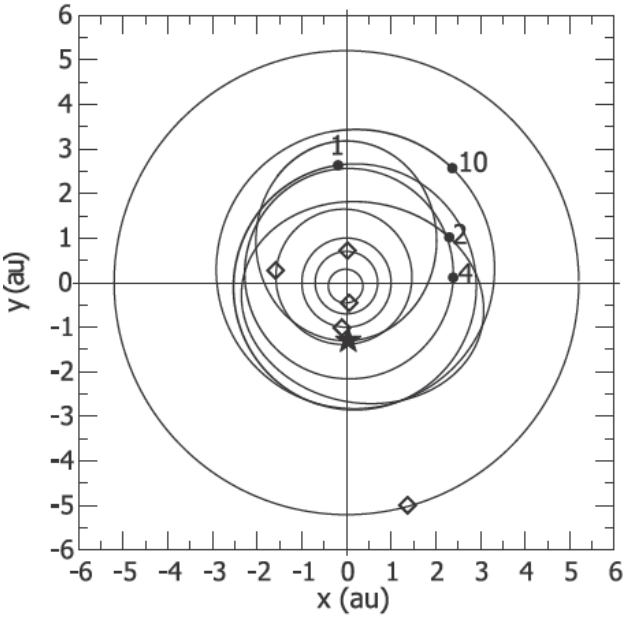

Figure 2. The orbit of 2008 LX16 in the ecliptic plane. The position of the planets, the asteroid 2008 LX16, dwarf planet (1) Ceres and three massive asteroids: (2) Pallas, (4) Vesta and (10) Hygiea are presented for the epoch 2008 June 15, *i.e.* for the date of first observation at Siding Spring Survey.

881806. The Baldone published nine observations of this asteroid.

The object 2008 LX16 was observed at three observational nights in April 2018. The asteroid moved at speed 0.11" per minute being 19.2 R magnitude object. It was independently discovered by the Baldone and by Pan-STARRS observatories at the opposition of 2018.

We computed the orbit of the asteroid 2008 LX16, one of the known MCs, based on all observations using the OrbFit software (http://adams.dm.unipi.it/~orbmaint/orbfit/). Sixteen perturbing massive asteroids and dwarf planet Pluto were used according to Farnocchia *et al.* (2013a,b) and similar to Wlodarczyk (2015).

We also used the new version of the OrbFit Software, namely OrbFit v.5.0.5, which has the new error model desribed in Chesley *et al.* (2010), as well as the debiasing and weighting scheme described in Farnocchia *et al.* (2015) called after that error model 2015 (see Table 4). Moreover, we used the DE431 version of JPL's planetary ephemerides. Recently, the possibility of calculating orbits according to the OrbFit software v.5.0.6 has appeared with implemented error model 2017, according to Vereš *et al.* (2017) (see Table 4).

Table 5 presents the starting orbital elements of the asteroid 2008 LX16 computed with the non-gravitational parameter $A2$. A positive value of $A2$ for asteroid 2008 LX16 denotes that the mean semimajor axis drifts da/dt>0 and hence the asteroid can be the prograde rotator. Table 5 shows that orbital elements have only changed a little, but $A2$ has also changed. Also, the error of all calculated orbital elements and $A2$ is smaller.

Table 5. Initial nominal orbital elements of the asteroid 2008 LX16 with different error models: a denotes semimajor axis, e - eccentricity, angles i, Ω and ω refer to the Equinox J2000.0, M - mean anomaly. Epoch JD2458400.5 TDB = 9 October 2018. Orbital elements are computed with the non-gravitational parameter $A2$.

a (au)	e	i (deg)	Ω (deg)	ω (deg)	M (deg)
error model 2015					
2.2410691	0.41891826	6.337966	70.535876	200.27248	26.704354
1.6E−06	3.9E−07	1.8E−05	8.2E−05	2.0E−04	4.7E−05
Orbital parameter: non-gravitational					
$A2$=(2.975±8.176)E−12 au/d^2					
error model 2017					
2.2410688	0.41891831	6.337966	70.535918	200.27248	26.704354
1.0E−06	2.0E−07	1.2E−05	4.8E−05	0.9E−04	1.5E−05
Orbital parameter: non-gravitational					
$A2$=(1.452±4.863)E−12 au/d^2					

Figure 2 presents the orbit of 2008 LX16 in the ecliptic plane. The position of the planets, the asteroid 2008 LX16, the dwarf planet (1) Ceres and three massive asteroids: (2) Pallas, (4) Vesta and (10) Hygiea are also presented for the epoch 2008 15 June, *i.e.* for the date of the first observation at Siding Spring Survey. According to the International Astronomical, a discoverer will be defined when the object is numbered, see https://minorplanetcenter.net/mpec/K10/K10U20.html.

4 2008 LX16 - Long time orbital evolution

To study the orbital evolution of asteroid 2008 LX16, we computed its Virtual Asteroids (VAs) with the use of the OrbFit software v. 5.0.5 and the method of Milani *et al.* (2005a,b). VAs, or variant orbits or clones denote swarm of orbits which lie somewhere in the *confidence region*. Each of these orbits fits well with observations. *Line of Variation* (*LOV*) is usually obtaining by fixing the value of all the orbital elements, six or seven when we used the Yarkovsky effect. Next, we changed only the mean anomaly. *LOV* is a one-dimensional part of a (curved) line in the initial conditions space generally computed with the uniform sampling of the *LOV* parameter. σLOV denotes the position along the Line of Variation, *LOV* in the σ space. Values of σ are usually in the interval (−3,3). *LOV* is used to compute multiple solutions which are useful in the orbit determination and their propagation (Milani *et al.* 2005a,b). We are computing 500 VAs on both sides of the nominal orbit on the *LOV* where the nominal orbit has $\sigma = 0$. Hence we have 1001 VAs. We computed 500 clones of both sides of the *LOV* with the uniform sampling of the *LOV* parameter. Then we propagate all the VAs 100 My forward.

Time evolutions of orbital elements of all clones are calculated using the software *swift_rmvs* developed by Levison and Levison (1994) This software takes into account the gravitational influence of all planets (variant *swift_rmvs*3_*f*), *i.e.* from Mercury to Neptune, and in the second case by adding four massive objects: dwarf planet (1) Ceres and three massive asteroids: (2) Pallas, (4) Vesta and (10) Hygiea. Our calculations were done for a case without the Yarkovsky effect.

Figure 3 presents the position of the remaining clones from the starting 1001 clones with $\sigma = 3$, of the asteroid 2008 LX16 after 100 My forward integration. Great star in Figure 3 presents the starting position of the nominal asteroid 2008 LX16. Small stars denote 30 remaining clones of 2008 LX16 using the old error model based on Farnocchia *et al.* (2015) and additional massive asteroids, (1) Ceres, (2) Pallas, (4) Vesta and (10) Hygiea (CPVH). The dots denote 45 remaining clones of 2008 LX16 using the same gravitational model, *i.e.* with CPVH and using the new error model based on Vereš *et al.* (2017). The open circles denote 46 remaining clones using the gravitational model without CPVH and with the new error model based on Vereš *et al.* (2017). It is visible that almost all remaining clones in phase space have orbits with aphelia smaller than the semimajor axes of Mars and perihelia larger to the semimajor axis of Venus.

In Figure 3 we can see that using the new error model, more clones remain in the Solar System model, *i.e.* 46 clones, in contrary to the old error model with 30 remaining clones. Probably we have a smaller dispersion of startup elements, *i.e.* smaller errors of these orbital elements - see Table 4. Furthermore, the number of clones remaining at the end of the integration period in the new Solar System model, hardly depends on the use of additional perturbing massive asteroids (CPVH).

It is visible that only several % of starting clones remain after 100 My integration. It can be explained by the fact that

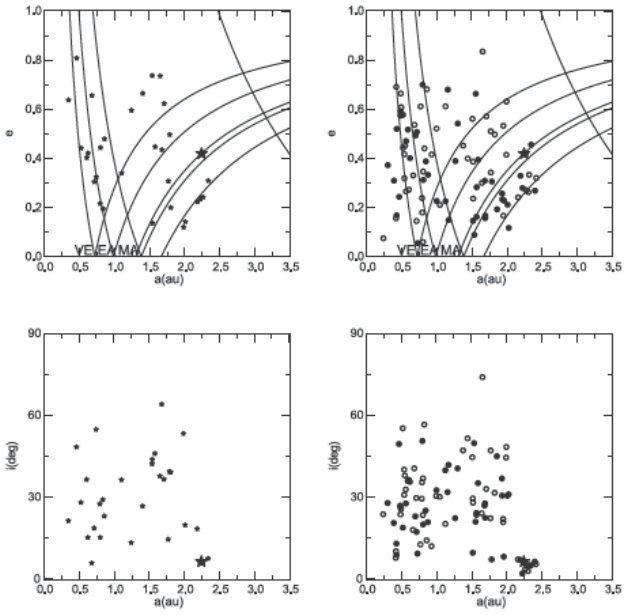

Figure 3. Remaining clones of 2008 LX16 after 100 My forward integration in the (a, e) plane - top panels and in the (a, i) plane - bottom panels. Small stars denote the position of clones with the use of the old error model based on Farnocchia *et al.* (2015) and with adding four massive bodies: (1) Ceres, (2) Pallas, (4) Vesta and (10) Hygiea (CPVH), dots - using the new error model based on Vereš *et al.* (2017) and with adding four massive bodies, CPVH, open circles denote positions of remaining clones computed without CPVH massive bodies and with the new error model. It is visible that almost all remaining clones in phase space have orbits with aphelia smaller than the semimajor axes of Mars and perihelia larger to the semimajor axis of Venus.

2008 LX16 is close to the line of the perihelion of the Earth. Generally, from all starting 1001 clones of the asteroid 2008 LX16 45% hit the Sun, (35÷38)% reached distance from the Sun greater than 1000 au, (13÷15)% have a collision with planets or perturbing massive asteroids, and (3÷5)% remain in the solar system, respectively.

5 2008 LX16 - Computation of the predicted theoretical meteor-stream radiant

Next, we computed theoretical meteor-stream radiant for asteroid 2008 LX16 according to the program of Neslusan *et al.* (1998). As the input parameters are orbital elements of the orbit of the parent body and its time of perihelion passage.

Results of computations are in Table 6 where:

- → date-max. - date of the predicted maximum [year, month, day]
- → dist. - distance between the Earth and parent body at the moment of the predicted maximum [au]
- → dt - time elapsed from the passage of the parent body through the point of its orbit nearest to the Earth's orbit at the investigated shower maximum (if negative, the body will pass the point after the maximum) [days]
- → alpha, delta - equatorial coordinates of radiant [degrees]
- → vg, vh - geocentric and heliocentric velocities [km/s]
- → l - solar longitude at the moment of predicted maximum [degrees]
- → min. dist. - the minimum distance between the given arc of the parent body and Earth's orbits [au]
- → d-disc. - the value of d-discriminant; d < 0.1 - good prediction, d > 0.5 - unreal prediction.

Table 6 shows that predicted theoretical meteor shower radiants will be visible at the turn of May and June in the following years.

Table 6. 2008 LX16. Computed theoretical meteor shower radiants.

date-max.	dist.	dt
date	au	days
2020 May 31.8	4.109	−512.0
2021 June 1.1	2.089	−147.0
2022 June 1.3	2.779	218.5
2023 June 1.6	4.189	583.7
2024 May 31.9	3.187	−276.4
alfa/delta	vg/vh	l
deg	km/s	deg
207.4/21.3	7.65/35.10	70.5
Equinox: 2000.0		
min. dist. = 0.2891 au; d-disc=0.307		

6 Summary

Between 2015 and 2018, 37 asteroids were discovered at the Baldone Astrophysical Observatory (MPC 069). We studied one of the interesting Mars-crosser (MC) observed at the Baldone Astrophysical Observatory, namely 2008 LX16. Also, NEO object 2006 VB14 and 1986 DA and 2014 LJ1 were observed. We computed orbits and analyzed the orbital evolution of these asteroids. 566 positions and photometric observations were obtained with Baldone Schmidt telescope in 2018 and 2019. We detected the rotation period, and other

physical characteristics of NEO objects 345705 (2006 VB14) and 6178 (1986 DA). We determined the rotational period of asteroid 6178 (1986DA), P=(3.12 ± 0.02)h.

Acknowledgment: We thank Julio A. Fernández and the anonymous reviewer for useful comments. We thank the Space Research Center of the Polish Academy of Sciences in Warsaw for the possibility to work on a computer cluster. We also thank L. Neslusan for his software. This research is funded by the Latvian Council of Science, project "Complex investigations of Solar System small bodies", project No. lzp-2018/1-0401. Kazimieras Cernis acknowledges the Europlanet 2024 RI project funded by the European Union's Horizon 2020 Research and Innovation Programme (Grant agreement No. 871149).

References

Chesley SR, Baer J, Monet DG. 2010. Treatment of star catalog biases in asteroid astrometric observations. Icar. 210(1):158–181.

Chesley SR, Farnocchia D, Nolan MC, Vokrouhlický D, Chodas PW, Milani A, et al. 2014. Orbit and bulk density of the OSIRIS-REx target Asteroid (101955) Bennu. Icar. 235(5):5-22.

Černis K, Wlodarczyk I, Eglitis I. 2015. Observational data and orbits of the asteroids discovered at the Baldone Observatory in 2008—2013. BaltA. (24): 251-262.

Eglitis I. 2019. Investigation of NEO asteroids 2006 VB14 and 1986 DA. OAP. 32(0):146–147.

Farnocchia D, Chesley SR, Vokrouhlický D, Milani A, Spoto F, Bottke WF. 2013a. Near Earth Asteroids with measurable Yarkovsky effect. Icar. 224(1):1–13.

Farnocchia D, Chesley SR, Chodas PW, Micheli M, Tholen DJ, Milani A, et al. 2013b. Yarkovsky-driven impact risk analysis for asteroid (99942) Apophis. Icar. 224(1):192–200.

Farnocchia D, Chesley SR, Chamberlin AB, Tholen DJ. 2015. Star catalog position and proper motion corrections in asteroid astrometry. Icar. 245:94–111.

Levison HF, Duncan MJ. 1994. The Long-Term Dynamical Behavior of Short-Period Comets. Icar. 108(1):18–36.

Milani A, Chesley SR, Sansaturio ME, Tommei G, Valsecchi GB. 2005a. Nonlinear impact monitoring: line of variation searches for impactors. Icar. 173(2):362–384.

Milani A, Sansaturio ME, Tommei G, Arratia O, Chesley SR. 2005b. Multiple solutions for asteroid orbits: Computational procedure and applications. A&A. 431:729-746

Neslusan L., Svoren J., Porubcan V. 1998. A computer program for calculation of a theoretical meteor-stream radian. A&A. 331:411-413

Skiff BA, Bowell E, Koehn BW, Sanborn JJ, McLelland KP, Warner BD. 2012. Lowell Observatory Near-Earth Asteroid Photometric Survey (NEAPS) - 2008 May through 2008 December. MPBu. 39:111–130.

Vereš P, Farnocchia D, Chesley SR, Chamberlin AB. 2017. Statistical analysis of astrometric errors for the most productive asteroid surveys. Icar. 296:139–149.

Wlodarczyk I. 2015. The Potentially Hazardous Asteroid (410777) 2009 FD. AcA. 65:215–231.

Wlodarczyk I. 2019a. Some parameters of selected NEAs. BlgAJ. 30: 44-59.

Wlodarczyk, I. 2019b. The potentially hazardous NEA 2001 BB1. Open Astronomy. 28:180–190.